

MODELING THE HARD STATES OF THREE BLACK HOLE CANDIDATES

HUI ZHANG^{1,2}, FENG YUAN¹, AND SYLVAIN CHATY³*Draft version June 8, 2010*

ABSTRACT

Simultaneous multiwavelength observations were recently performed for three black hole candidates — SWIFT J1753.5-0127, GRO J1655-40 and XTE J1720-318. In this paper, we test the accretion-jet model originally proposed for XTE J1118+480 by investigating the hard state of these three sources using this model. The accretion flow in the model is composed of an inner hot accretion flow and an outer truncated thin disk. We find that the model satisfactorily explains the spectrum ranging from radio to X-rays, with the radio and X-ray spectra dominated by the synchrotron and thermal Comptonization emissions in the jet and the hot accretion flow, respectively, while the infrared and optical being the sum of the emissions from the jet, hot accretion flow, and the truncated thin disk. Similar to the case of XTE J1118+480, the model can also explain, although only qualitatively in some cases, the observed timing features including quasi-periodic oscillation, and positive and negative time lags between the optical and X-ray emissions detected in SWIFT J1753.5-0127. The origin of the ejection events detected in XTE J1720-318 is also briefly discussed.

Subject headings: accretion, accretion disks — black hole physics—ISM: jets and outflows—stars: individual (SWIFT J1753.5-0127, GRO J1655-40, XTE J1720-318)

1. INTRODUCTION

More than 40 black hole X-ray binaries or candidate black-hole X-ray binaries have been found so far (1) Because they are closer to us and the black hole mass is much smaller compared to active galactic nuclei (AGNs), they supply us with some unique information that is very valuable to understand the physics of accretion onto compact objects, particularly black holes. These information include simultaneous multiwaveband spectral energy distribution (SED), the state transition (see below), timing features such as quasi-periodic oscillation (QPO), and time lags between different wavebands. For complete reviews on observations and theory of black hole X-ray binaries, the readers can refer to McClintock & Remillard (2006), Fender (2006), Zdziarski & Gierlinski (2004), and Done, Gierlinski & Kubota (2007). Here we only briefly introduce some of the most relevant background.

Black hole X-ray binaries are usually thought to come into five different states, namely quiescent, low/hard (LHS), high/soft (HSS), intermediate, and very high (or steep power-law) states. We focus on LHS in this paper. The quiescent state is generally assumed to be the low-luminosity version of the LHS. The HSS state, which is relatively well understood, is described by a standard thin disk sandwiched by a corona. The steep power-law state or intermediate state is still poorly understood, although some hard efforts have been made (e.g., Kubota & Done 2004; Done & Kubota 2006).

One of the key mysteries of LHS has been the origin of the hard X-ray emission, since the standard thin disk

is too cool to emit hard X-rays. One traditional explanation is from a hot corona above and below a standard thin disk. The disk corona is hot due to heating by reconnection of the magnetic field emerged from the underlying disk due to Parker instability, like in the case of solar corona (e.g., Liang & Price 1977; Galeev, Rosner, & Vaiana 1979). If this is the model of the LHS (e.g., Haardt & Maraschi 1993), we need to answer why the hard X-ray emission in HSS is much weaker even though the same process should also be happening in this case. Unfortunately, while the scenario of this model is very attractive, our current poor knowledge of magnetic reconnection hampers us from a deeper quantitative study. The only MHD numerical simulation of thin disk based on shearing-box approximation with self-consistent turbulent dissipation, radiative transfer, and radiative cooling tentatively indicates that the corona may be too weak and temperature too low to produce the observed hard X-ray emission (Hirose, Krolik & Stone 2006). In addition to the disk-corona model, another type of model for LHS is the pure jet model. In its early version it was proposed that both radio and X-ray emissions originate from the synchrotron emission of the jet (Markoff, Falcke & Fender 2001). Because the observed shape of the high-energy cutoff cannot be easily fit by the synchrotron emission (Zdziarski et al. 2003), the jet model evolved subsequently and now the X-ray emission is proposed to be produced by the synchrotron-self-Compton process in the “jet base” (Markoff, Nowak & Wilms 2005). This model has been applied to the LHS of other sources in addition to XTE J1118+480 (Markoff, Falcke & Fender 2001), including GRO J1655-40, which will be studied in this paper (Migliari et al. 2007). “However, Maccarone (2005) argue that the X-rays were unlikely to be formed in jets by the comparison of the properties of accreting black holes and accretion neutron stars. Maitra et al. (2009) and Malzac, Belmont & Fabian (2009) show that the revised jet model by Markoff et al. (2005) also possesses pair-production problem for bright sources.”

¹ Key Laboratory for Research in Galaxies and Cosmology, Shanghai Astronomical Observatory, Chinese Academy of Sciences, 80 Nandan Road, Shanghai 200030, China; fyuan@shao.ac.cn

² Graduate School of the Chinese Academy of Sciences, Beijing 100039, China

³ AIM - Astrophysique Interactions Multi-échelles (UMR 7158 CEA/CNRS/Université Paris 7 Denis Diderot), CEA Saclay, DSM/IRFU/Service d’Astrophysique, Bât. 709, L’Orme des Merisiers, FR-91 191 Gif-sur-Yvette Cedex, France

In this paper, we focus on the hot accretion flow model. In this model, the X-ray emission is produced by a hot accretion flow via thermal Comptonization process. The most well-known hot accretion flow model is the advection-dominated accretion flow (ADAF; Ichimaru 1977; Rees et al. 1982; Narayan & Yi 1994, 1995; Abramowicz et al. 1995). The ADAF model, or more generally hot accretion flow model, has drawn intensive theoretical interests and has been successfully applied to many low-luminosity sources since its discovery. It is the only dynamically based accretion model to be able to produce hard X-ray emissions (see Narayan & McClintock 2008 and Yuan 2007 for recent reviews). Esin, McClintock & Narayan (1997) applied the ADAF model in detail to Nova Muscae 1991 and successfully modeled its low-hard and quiescent states. In their model a standard thin disk is truncated at a “transition” radius and replaced by an inner ADAF. The best evidence for the truncation of thin disk is perhaps the UV spectrum of XTE J1118+480 (Esin et al. 2001; Frontera et al. 2001; Chaty et al. 2003; Yuan, Cui & Narayan 2005, hereafter YCN05. See Ho 2002 and Yuan 2007 for review of evidences for the truncated disk in low-luminosity AGNs), which can only be fitted by a truncated thin disk. However, this model significantly underestimates the radio and infrared spectra (Esin et al. 2001). This is not surprising since we now know that LHS is usually associated with jets (Fender 2006) while they are not included in Esin et al. (2001).

YCN05 extended the work of Esin et al. (1997; 2001) by including a jet and applied this accretion-jet model (see Section 2 for the description of the model) to XTE J1118+480 again because this source has so far the best simultaneous multiwaveband data, including SED and various kinds of timing features that supply good constraints to theoretical models. In the interpretation of YCN05, the X-rays come from the accretion flow (ADAF), while the radio and most of the IR radiation come from the jet. The model not only successfully explains the SED, but also the timing features including QPOs and the otherwise puzzling “negative” and “positive” time lags between optical/UV and X-rays (see also similar work by Malzac et al. 2004). The QPO interpretation requires the existence of the geometrically thick ADAF bounded at a certain radius while the interpretation of time lags requires that both the jet and the ADAF contribute to the IR and optical radiation, both of which are natural components or results of the accretion-jet model.

An additional constraint comes from the radio-X-ray correlation found in black hole X-ray binaries, and more generally, in black hole sources (Gallo et al. 2003; Corbel et al. 2003; Merloni et al. 2003; Falcke, Körding, & Markoff 2004; Gültekin et al. 2009; but see Xue & Cui 2007 for a different point of view). This correlation is well explained by the accretion-jet model (Yuan & Cui 2005). Moreover, Yuan & Cui (2005) made two predictions. One is that when the X-ray luminosity of the system is lower than $L_{\text{crit}} \sim 10^{-6} L_{\text{Edd}}$, the correlation should steepen, with the correlation index changing from ~ 0.6 to ~ 1.23 . Another prediction is that below L_{crit} the X-ray emission of the system should be dominated by the jet. Both predictions have recently obtained strong supports in both observational and theoretical aspects (see review

by Yuan et al. 2009c). Especially, Yuan et al. (2009c) combined the radio and X-ray luminosity of 22 AGNs satisfying $L_x \lesssim L_{\text{crit}}$ and found that the correlation index is indeed ~ 1.22 , which is in excellent agreement with the prediction of Yuan & Cui (2005).

The coupled ADAF-jet model has only been applied to two sources so far, XTE J1118+480 (YCN05) and XTE J1550-564 (Yuan et al. 2007). Thus, it is necessary to test the model on a larger sample. Recently some new black hole candidates have been found and some of them have very good simultaneous multiwavelength data. In this paper, we first overview the accretion-jet model in Section 2, we then study the LHS of three such sources, namely SWIFT J1753.5-0127, GRO J1655-40, and XTE J1720-318, by using the main observational constraints including SED, QPO, and time lags between different bands in Section 3. In Section 4, we summarize our main results.

2. THE ACCRETION-JET MODEL

We briefly describe the ADAF-jet model here. The readers can refer to YCN05 for additional details. In this model, the accretion flow at large radii is described by a standard thin disk. It makes a transition at R_{tr} and becomes a hot accretion flow (ADAF). Both observational (Yuan & Narayan 2004) and direct theoretical (“evaporation” mechanism: Liu et al. 1999; Różańska & Czerny 2000; “turbulent diffusion” mechanism: Manmoto & Kato 2000) studies indicate that the value of R_{tr} increases with the decrease of accretion rate, although their quantitative results are different. Numerical simulations of hot accretion flow have shown that the flow is convectively unstable, irrespective of whether the radiation is weak (e.g., Igumenshchev & Abramowicz 1999; Stone, Pringle & Begelman 1999; 2001) or strong (Yuan & Bu 2010). As a result, the accretion rate decreases inward because the gas circulates in the convective eddies. To mimic this effect, we parameterize the accretion rate with a parameter s , $\dot{M} = \dot{M}_{\text{out}}(R/R_{\text{tr}})^s$, where \dot{M}_{out} is the accretion rate at the outer boundary of the hot accretion flow R_{tr} and s describes the strength of the outflow. For the viscous parameter α and magnetic parameter β (defined as the ratio of gas pressure to the sum of gas and magnetic pressure), we set $\alpha = 0.3$ and $\beta = 0.9$ as suggested by MHD numerical simulations (Hawley & Krolik 2001). Hence they are not free parameters in our model. Another parameter is δ , the fraction of the turbulent dissipation that directly heats the electrons. The values of δ and s are well constrained in the case of our Galactic center supermassive black hole, Sgr A* (Yuan et al. 2003), which are $\delta = 0.5$ and $s = 0.3$. However, we want to emphasize that large uncertainties exist in their values. For example, some numerical simulations indicate moderately smaller δ ($\sim (T_e/T_i)^{1/2}$: Sharma et al. 2007) and larger s ($0.5 \lesssim s \lesssim 1$: Stone & Pringle 2001). We therefore also try other values. The radiative processes in hot accretion flow include synchrotron, bremsstrahlung, and their Comptonization. We first solve for the global dynamical solution of the hot accretion flow to obtain the physical quantities such as density, ion and electron temperature, and magnetic field. We then calculate the radiative transfer to obtain the emitted spectrum. The details of the calculation can be found in Yuan et al. (2003). Specifically, the X-ray radiation is typically dom-

inated by thermal Comptonization for most of the accretion rates of interest.

The model of jet radiation is based on the internal shock scenario, which has also been widely adopted in the study of gamma-ray bursts. A small fraction of the material in the accretion flow, described by \dot{M}_{jet} , is transferred into the vertical direction and forms a jet. The jet is assumed to have a conical geometry with a half-open angle ϕ and a bulk Lorentz factor Γ_{jet} . We fix those values to be $\phi = 0.1$ and $\Gamma_{\text{jet}} = 1.2$, thus they are not free parameters. A larger ϕ will decrease the total flux, but this impact can be absorbed by the accretion rate. Γ_{jet} is well within the range obtained by combining observations and numerical simulations: $\Gamma_{\text{jet}} \leq 1.67$ (Gallo et al. 2003). A small fraction of the electrons in the jet are accelerated by the internal shocks and form a power-law energy distribution with index p . The energy density of accelerated electrons and amplified magnetic field in the shock front is determined by two free parameters, ϵ_e and ϵ_B , defined as the ratio of the electron energy and magnetic energy to the shock energy, respectively. Only synchrotron emission is considered since Compton scattering is not important in our model (Markoff, Falcke & Fender 2001; Wu, Yuan & Cao 2007). The radio and X-ray radiation comes from the optically thick and optically thin synchrotron emission of the accelerated electrons, respectively.

The main advantage of the accretion-jet model is that it has strong dynamical basis, such as the thin disk, hot accretion flow, and the transition between them. We would like to point out, however, that large uncertainties exist in our model since many simplifications and assumptions have to be adopted in current models of accretion flow and jet. First, accretion flows are intrinsically three-dimensional but we so far can only get global solution under one-dimensional approximation. Second, the exact value of the viscous parameter α is still unknown and it must be a function of radius. It very likely originates from the stress of the magnetic field amplified by Magneto-Rotational Instability (MRI) (Balbus & Hawley 1998). MHD numerical simulation can produce some values but they depend on, e.g., initial magnetic field configuration which is unclear. Third, general relativity effect, which is important in the inner region of the accretion flow and the jet, is usually also neglected. Fourth, when calculating Comptonization, almost all current work consider only local scattering while the global effect is neglected (Yuan et al. 2009b; Xie et al. 2010). Fifth, the jet model is even worse; the formation and collimation mechanisms of jet are still not solved, even the ingredient of the jet is debated. In spite of the above caveats, all the above effects are of higher order and we believe that our current models can present valuable information when we compare their prediction with observations. On the other hand, given these model uncertainties, we think that it is physically not appropriate to do fine statistical analysis such as χ^2 analysis when comparing the theoretical prediction with data as adopted in some works (e.g., Migliari et al. 2007). When judging the goodness of the modeling, we have to be satisfied with comparison by eye. But in Section 3.4 we do show the effects of changing the main model parameters, which are \dot{M} , δ , s , and \dot{M}_{jet} .

3. MODELING THE THREE SOURCES

3.1. *SWIFT J1753.5-0127*

3.1.1. *Spectrum*

SWIFT J1753.5-0127 was discovered on 2005 May 30 when it underwent an X-ray outburst. According to its spectrum and timing, this source is regarded as a good black hole candidate (e.g., Miller et al. 2006; Ramadevi & Seetha 2007; Zhang et al. 2007; Cadolle Bel et al. 2007). Simultaneous multiwavelength observations were performed with *International Gamma-Ray Astrophysics Laboratory (INTEGRAL)*, *RXTE*, New Technology Telescope (NTT), Rapid Eye Mount Telescope, and Very Large Array (VLA) on 2005 August 10-12, and a good multiwaveband spectrum was obtained (Cadolle Bel et al. 2007). The data obtained on August 11 are shown in Figure 1, which are taken from Cadolle Bel et al. (2007).

It is still difficult to determine the accurate parameters, such as mass, distance and inclination angle of this source, so following Cadolle Bel et al. (2007), we set the distance of the source $d = 6$ kpc, the mass of the black hole $M = 9M_{\odot}$, and the inclination angle of the source to be 63° . Changing these parameters will have different effects on our modeling results. A larger value of the inclination angle will make the emission from the jet weaker, but most of this effect can be absorbed by the mass-loss rate in the jet. A larger M or smaller d will make the accretion rate smaller thus the predicted spectrum softer, if all other model parameters are kept fixed. We then calculate the emitted spectrum from the ADAF and jet as described above. The top panel of Figure 1 shows our best modeling results. The values of parameters adopted are $\dot{M} = 0.1\dot{M}_{\text{Edd}} \equiv L_{\text{Edd}}/c^2$, $s = 0.3$, $\delta = 0.5$, $R_{\text{tr}} = 250 R_s$, $\dot{M}_{\text{jet}} = 8 \times 10^{-5}\dot{M}_{\text{Edd}}$, $\epsilon_e = 0.04$, $\epsilon_B = 0.02$, and $p = 2.1$. We can see from the figure that, similar to XTE J1118+480 (YCN05) and XTE J1550-564 (Yuan et al. 2007), the radio and X-ray emissions are dominated by the jet and the ADAF, respectively, while the infrared (IR) and optical are the sum of the emissions from the jet, ADAF, and the truncated thin disk. Given that both accretion flow and jet models have large uncertainties and some approximations have to be adopted, as we have stated in Section 2, we think it is unreasonable to do elaborate statistical analysis as was done in Migliari et al. (2007). To show the “goodness” of the fitting we present the ratio of the observed flux and the theoretical prediction in the bottom panel of Figure 1 (and Figures 2 and 3 as well). For the observed flux, we simply adopt the middle value but neglect their errorbar. We feel the modeling results are satisfactory.

3.1.2. *Timing features: QPO and the time lags between optical and X-ray emissions*

A low-frequency QPO was clearly detected and its frequency is 0.241 Hz on August 11 (Cadolle Bel et al. 2007). The QPO frequency is found to correlate with the X-ray flux almost linearly (Zhang et al. 2007; Ramadevi & Seetha 2007). Such a correlation seems to be common in black hole X-ray binaries (e.g., Cui et al. 1999 for XTE J1550-564).

Many models of QPO have been proposed. Especially, for the accretion configuration of our model, namely an inner hot accretion flow plus an outer truncated thin disk,

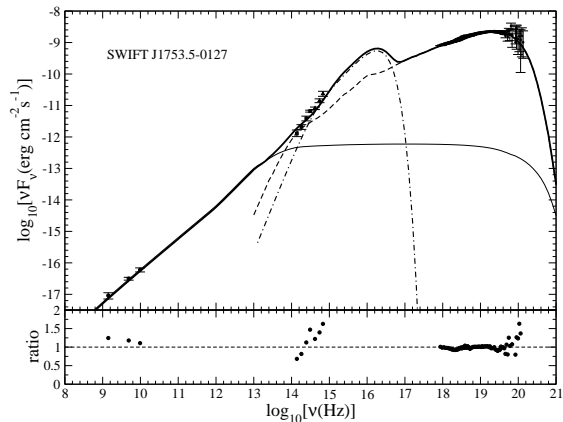


FIG. 1.— SED of SWIFT J1753.5-0127. *Top*: the dash-dotted, dashed, and thin solid lines show the emissions of the truncated thin disk, the hot accretion flow, and the jet, respectively. The thick solid line shows their sum. *Bottom*: ratio of the observed flux and the theoretical value.

Giannios & Spruit (2004; see also Rezzolla et al. 2003) suggested that the QPO can be excited by the interaction of ADAF and the thin disk and resulted from the basic p -mode oscillations of the inner ADAF, with a frequency near the Keplerian frequency at R_{tr} . The Keplerian frequency at $R_{tr} = 250 R_s$ is 0.32 Hz, which is close to the observed QPO frequency of 0.24 Hz. During the outburst, the decrease of the accretion rate results in the decrease of the X-ray flux. Since the value of R_{tr} increases (thus the Keplerian frequency at R_{tr} decreases) in this process, as introduced in Section 2, this qualitatively explains the detected correlation between the QPO frequency and the X-ray flux.

Durant et al. (2008) conducted simultaneous optical and X-ray observations and did cross-correlation analysis. They found that the optical emission *decreases* a few seconds *before* the X-rays *increase*. In addition to this “negative time lag” or “precognition dip”, the cross-correlation function also shows a weaker “positive lag”, which means that the optical emission lags the X-rays by several seconds. These positive and negative lags are similar to XTE J1118+480, but the timescales of these two lags are markedly different. For XTE J1118+480, the precognition dip or negative lag is weaker while the positive lag is stronger (Kanbach et al. 2001).

The two time lags in XTE J1118+480 have been explained by the accretion-jet model in YCN05. The same mechanism works for SWIFT J1753.5-0127. From Figure 1, we can see that both ADAF and the jet contribute to the optical emission. When there is a perturbation such as a sudden increase of accretion rate, it will first propagate in ADAF, then into the jet. The increase of accretion rate and subsequently the increase of mass-loss rate in the jet will result in an increase of X-ray emission from ADAF and subsequently an increase of optical emission from the jet. This is the reason for the positive lag. On the other hand, ADAF emits both optical and X-ray emissions. The optical emission originates from the self-absorbed synchrotron emission, which depends on the profiles of T_e and optical depth. For the specific parameters of the hot accretion flow in SWIFT J1753.5-

0127, we find that an *increase* of \dot{M} results in a *decrease* of the optical flux. Since optical emission comes from $\sim 40 R_s$ while the X-rays from $\sim 10 R_s$, an increase of \dot{M} first results in a decrease of optical flux then an increase of X-ray flux after the accretion timescale at $\sim 40 R_s$. This could be the reason for the negative lag.

The next question is why the intensity of the two time lags are opposite. This is because of the differences in the model parameters. The value of \dot{M} in SWIFT J1753.5-0127 is higher than that in XTE J1118+480 ($\dot{M} = 0.05 \dot{M}_{Edd}$), while \dot{M}_{jet} is lower than XTE J1118+480 ($\dot{M}_{jet} = 2.5 \times 10^{-4} \dot{M}_{Edd}$). Comparing Figure 1 in this paper with Figure 2 in YCN05, we can see that this results in a significantly smaller relative contribution of the jet compared to ADAF in SWIFT J1753.5-0127 than in XTE J1118+480. This is why the intensities of the “positive” and “negative” correlation are opposite between the two sources.

Quantitatively, however, we can only explain the positive time lag. The optical emission in the jet mainly comes from $d \sim 7000 R_s$. The X-ray emission from ADAF originates from $\lesssim 10 R_s$. So the timescale of the positive lag is determined by $d/c \sim 1.5s$, which roughly agrees with the observation. On the other hand, the optical emission by ADAF mainly comes from $\sim 40 R_s$. Thus the timescale of the negative lag is determined by the accretion timescale there, which is $\sim 0.2s$. This is much shorter than the detected timescale of several seconds. We speculate that the discrepancy may be due to the following reasons. For technical reasons, when solving for the global solution of ADAF, we have to set the angular velocity at R_{tr} to be substantially sub-Keplerian, although it should be super-Keplerian there. This makes the radial velocity of the accretion flow much larger than it should be and thus the accretion time scale is much shorter. Another possible reason is that we choose the viscous parameter $\alpha = 0.3$ in our calculations, but the actual value may be significantly smaller.

3.2. GRO J1655-40

GRO J1655-40 entered a new outburst in 2005 February after seven years of quiescence and many observations have been conducted then (e.g., Shaposhnikov et al. 2007; Caballero-García et al. 2007; Joinet, Kalemci, & Senziani 2008) especially a simultaneous multiwavelength campaign by *RXTE*, *INTEGRAL*, *SMART*, *VLA*, and *Spitzer* (Migliari et al. 2007). We make use of the multiwavelength data obtained on September 24 when the source was in the “standard” LHS, as shown in Figure 2. The details of observations and data analysis can be found in Migliari et al. (2007). A QPO with frequency of 0.3 Hz was also found that day (Migliari et al. 2007).

To model this source, we adopt the mass of the black hole $M = 6.3 M_\odot$ (Greene et al. 2001), and the distance $D = 3.2$ kpc (Hjellming & Rupen 1995). The inclination angle of the accretion disk is $69^\circ.50 \pm 0^\circ.08$ (Orosz & Bailyn 1997), while Greene obtained $70^\circ.2 \pm 1^\circ.9$ (Greene et al. 2001). So we set the inclination angle of this source to be 70° in this paper. Other values of mass and inclination angle are reported by Beer & Podsiadlowski (2002), but their values do not deviate too much from our values adopted here and will not impact our final result seriously. The inclination angle of the jet is $85^\circ \pm 2^\circ$

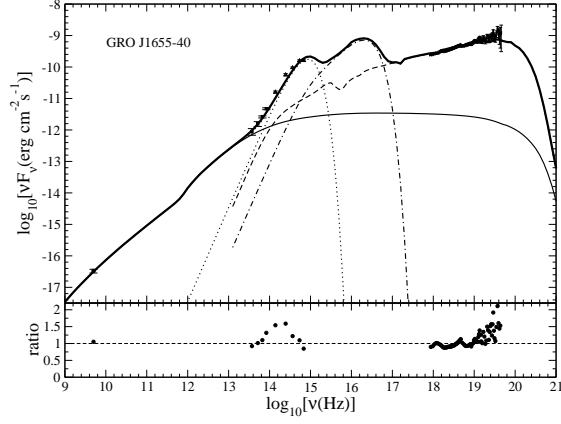


FIG. 2.— SED of GRO J1655-40. *Top*: the dash-dotted, dashed, and thin solid lines show the emissions of the truncated thin disk, the hot accretion flow, and the jet, respectively. The dotted line shows the blackbody emission of the companion star. The thick solid line shows their sum. *Bottom*: the ratio of the observed flux and the theoretical value.

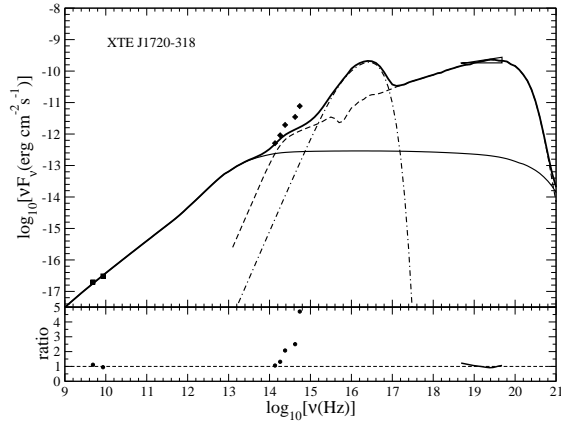


FIG. 3.— SED of XTE J1720-318. *Top*: the dash-dotted, dashed, and thin solid lines show the emissions of the truncated thin disk, the hot accretion flow, and the jet, respectively. The thick solid line shows their sum. Note the contribution from the companion star has not been subtracted in the data. *Bottom*: ratio of the observed flux and the theoretical value.

(Hjellming & Rupen 1995), which means that the jet is not perpendicular to the disk, and here we set the inclination angle of the jet to be 85° for jet modeling.

Figure 2 shows the modeling result of the spectrum. In addition to the accretion flow and jet, also shown in the figure is the emission from the possible companion star, since the impact of the companion star has not been subtracted. The model parameters are $\dot{M} = 0.06\dot{M}_{\text{Edd}}$, $R_{\text{tr}} = 200 R_s$, $s = \delta = 0.3$, $\dot{M}_{\text{jet}} = 2 \times 10^{-4}\dot{M}_{\text{Edd}}$, $\epsilon_e = 0.06$, $\epsilon_B = 0.02$, and $p = 2.1$. Again, the radio and X-ray emissions are dominated by the jet and ADAF, respectively. The IR and optical emissions are the sum of the emissions of the jet, ADAF, truncated thin disk, and the companion star.

The Keplerian frequency at $R_{\text{tr}} = 200 R_s$ is $\sim 0.45\text{Hz}$, which is roughly consistent with the frequency of the detected QPO.

3.3. XTE J1720-318

3.3.1. Spectrum

XTE J1720-318 is a black hole candidate discovered in 2003. Nearly simultaneous multiwavelength observations were conducted during its outburst in 2003 with VLA in radio (April 26; Brocksopp et al. 2005), NTT and SOFI in optical and IR (April 24 and 27; Chaty & Bessolaz 2006), and *INTEGRAL* in X-ray (April 6-22; Cadolle Bel et al. 2004). The spectrum is shown in Figure 3. Note that the contribution from the companion star has not been subtracted.

Following Cadolle Bel et al. (2004) and Chaty & Bessolaz (2006), we assume the mass of the black hole, distance, and inclination angle to be $M = 5M_\odot$, $d = 8\text{ kpc}$ and $i = 60^\circ$, respectively. Figure 3 shows the modeling results. The model parameters are $\dot{M} = 0.08\dot{M}_{\text{Edd}}$, $s = \delta = 0.5$, $R_{\text{tr}} = 150 R_s$, $\dot{M}_{\text{jet}} = 6 \times 10^{-5}\dot{M}_{\text{Edd}}$, $\epsilon_e = 0.06$, $\epsilon_B = 0.08$, and $p = 2.1$. The modeling results are similar to the other two sources, i.e. the radio and X-ray emissions are dominated by the jet and ADAF, respectively.

3.3.2. Ejection events

An interesting result from radio observation is that two ejection events took place, possibly associated with the state transition from hard to soft (Brocksopp et al. 2005). The spectral analysis indicates that the radio-emitting material expands and becomes optically thin from optically thick. Actually such kind of episodic ejection of material seems to be common during the transition from hard to soft states (see review in Fender, Belloni & Gallo 2004). The ejection is regarded as a “type-II” jet and its features are reviewed in detail in Fender & Belloni (2004). An interesting question is then whether we can explain these ejection events in the framework of the accretion-jet model?

The formation of continuous jet or “type-I” jet has been the topic of intensive study for many years and we now have relatively good understanding of it. Briefly, the formation of this kind of jet is due to the extraction of the rotation energy of the spinning black hole (Blandford & Znajek 1977) or the accretion disk (Blandford & Payne 1982) by a large-scale *open* magnetic field. In contrast, we have little knowledge of the formation of episodic jets. Very recently, by analogy with the “coronal mass ejection” theory in solar physics, Yuan et al. (2009a) proposed that the formation of episodic jets is due to the extraction of rotation energy of the accretion flow by the *closed* magnetic field amplified in the disk and emerged into the corona. During the transition from LHS to HSS, the hot accretion flow collapses and forms a thin disk due to the strong cooling. In this process, a large amount of magnetic flux emerges out of the accretion flow in a very short timescale and some coronal material is pushed outward by the strong magnetic pressure force. For details, the readers can refer to Yuan et al. (2009a).

3.4. The effects of changing model parameters

As introduced in Section 2, the main free parameters of our model are \dot{M} , δ , s and \dot{M}_{jet} . It is therefore interesting to see how the modeling results (i.e., the predicted spectrum) will change when these parameters are changed. Based on the “best” model of each source as shown in Figures 1-3, we change one of the above four parameters each time by a larger and smaller value compared to the

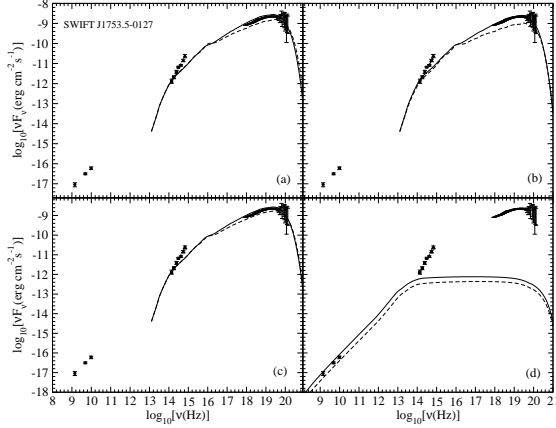


FIG. 4.— Effects of changing main model parameters for SWIFT J1753.5-0127. Each panel shows the larger and smaller parameters than the “best” one. Panel (a): $\dot{M} = 0.105\dot{M}_{\text{Edd}}$ (solid line) and $\dot{M} = 0.09\dot{M}_{\text{Edd}}$ (dashed line). Panel (b): $\delta = 0.6$ (solid line) and $\delta = 0.3$ (dashed line). Panel (c): $s = 0.2$ (solid line) and $s = 0.5$ (dashed line). Panel (d): $\dot{M}_{\text{jet}} = 10^{-4}\dot{M}_{\text{Edd}}$ (solid line) and $\dot{M}_{\text{jet}} = 6 \times 10^{-5}\dot{M}_{\text{Edd}}$ (dashed line).

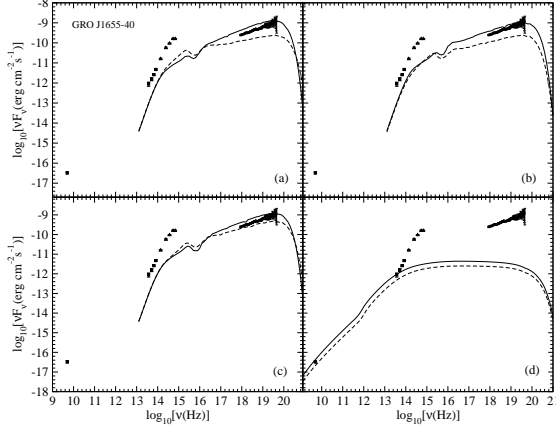


FIG. 5.— Effects of changing main model parameters for GRO J1655-40. Each panel shows the larger and smaller parameters than the “best” one. Panel (a): $\dot{M} = 0.07\dot{M}_{\text{Edd}}$ (solid line) and $\dot{M} = 0.05\dot{M}_{\text{Edd}}$ (dashed line). Panel (b): $\delta = 0.5$ (solid line) and $\delta = 0.1$ (dashed line). Panel (c): $s = 0.1$ (solid line) and $s = 0.5$ (dashed line). Panel (d): $\dot{M}_{\text{jet}} = 2.5 \times 10^{-4}\dot{M}_{\text{Edd}}$ (solid line) and $\dot{M}_{\text{jet}} = 1.5 \times 10^{-4}\dot{M}_{\text{Edd}}$ (dashed line).

“best” value of the model, but keep all other parameters the same. We calculate the emitted spectra and show the results in Figures 4-6 for the three sources. As we expect, a higher \dot{M} , δ , \dot{M}_{jet} and a lower s will result in a higher emitted flux, a lower \dot{M} , δ , \dot{M}_{jet} , and a higher s will result in a lower emitted flux. The difference of the lines in each figure gives us an idea of the dependence or sensitivity of the modeling result on the parameters.

4. SUMMARY AND DISCUSSION

YCN05 proposed an accretion-jet model for the LHS of XTE J1118+480. In this model the outer thin disk makes a transition at R_{tr} and becomes a hot accretion flow. At the innermost region some fraction of the accretion gas is transferred into the vertical direction and forms a jet. This model successfully explained the spectral and timing features of XTE J1118+480 (YCN05)

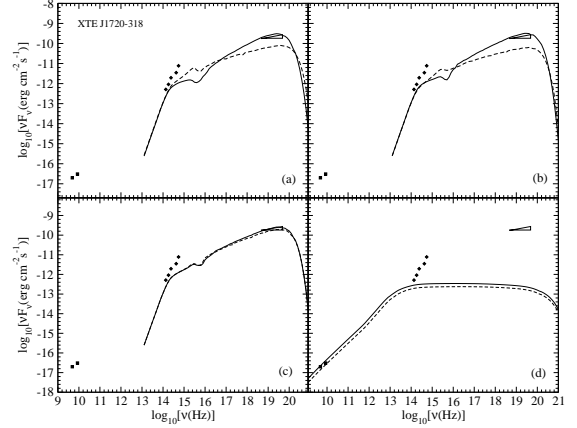


FIG. 6.— Effects of changing main model parameters for XTE J1720-318. Each panel shows the larger and smaller parameters than the “best” one. Panel (a): $\dot{M} = 0.09\dot{M}_{\text{Edd}}$ (solid line) and $\dot{M} = 0.07\dot{M}_{\text{Edd}}$ (dashed line). Panel (b): $\delta = 0.6$ (solid line) and $\delta = 0.3$ (dashed line). Panel (c): $s = 0.3$ (solid line) and $s = 0.6$ (dashed line). Panel (d): $\dot{M}_{\text{jet}} = 7 \times 10^{-5}\dot{M}_{\text{Edd}}$ (solid line) and $\dot{M}_{\text{jet}} = 5 \times 10^{-5}\dot{M}_{\text{Edd}}$ (dashed line).

and XTE J1550-564 (Yuan et al. 2007). In this paper we apply the model to three additional sources, namely SWIFT J1753.5-0127, GRO J1655-40, and XTE J1720-318, for which we have new simultaneous multiwaveband spectral and timing data. Similar to our previous results, we find that the radio and X-ray spectra are dominated by the synchrotron emission from the jet and the thermal Comptonization in the hot accretion flow, respectively; while the IR and optical emissions are the sum of emissions of the jet, ADAF, and the truncated thin disk. The QPO is explained by the oscillation of ADAF, with the QPO frequency close to the Keplerian frequency at R_{tr} . The “positive” and “negative” time lags between optical and X-ray radiations can also be explained by the model, although only qualitatively so far in the case of the “negative lag” (Section 3.1.2).

SWIFT J1753.5-0127 and XTE J1720-318 are two of the so-called outliers to the radio/X-ray correlation, in the sense that their radio emission is very weak compared to their X-ray emission. The radio luminosity of these two sources is ~ 2 and 3 orders of magnitude lower respectively than that predicted by the general radio/X-ray correlation introduced in Section 1 and their X-ray luminosity. This is reflected by the lower ratio of \dot{M}_{jet} and \dot{M} compared to that of GRO J1655-40. We speculate that this indicates that the spin of the black holes, a , in these two sources is small compared to other sources. This makes the jets very weak since it has been shown that jet power is proportional to a^4 or even a^6 (Tchekhovskoy, Narayan & McKinney 2010; but see also Fender, Gallo & Russell 2010).

Miller et al. (2006) analyzed the high-resolution spectral data of the LHS of Swift J1753.5-0127 and found a soft or thermal component when the 0.5-10 keV luminosity is higher than $\sim 3 \times 10^{-3}L_{\text{Edd}}$. They interpret it as the emission of a standard thin disk extending to the innermost stable circular orbit (ISCO). This conclusion, however, is currently debated. Gierlinski, Done & Page (2008) analyzed the same data set of a source and showed

that the spectrum can also be fitted without the need for a thermal component. Hiemstra et al. (2009) tested more spectral models than Miller et al. and concluded that several models can fit the data without the need for the thermal component. Even though the data analysis of Miller et al. is correct, the existence of a thermal component does not necessarily imply that the thin disk must extend to the ISCO. This is because the component could also originate from some cold clumps embedded in the hot accretion flow, formed due to thermal instability when the accretion rate is higher than roughly the critical accretion rate of an ADAF $\sim \alpha^2 \dot{M}_{\text{Edd}} \equiv \alpha^2 10 L_{\text{Edd}}/c^2$ (Yuan 2003; Yuan et al. 2007); or from a small inner disk, formed due to the strong cooling and condensation

of the hot accretion flow (Liu et al. 2007; Taam et al. 2008).

We thank M. Cadolle Bel and S. Migliari for providing us with the data for SWIFT J1753.5-0127 and GRO J1655-40, respectively. We also thank the second referee's constructive suggestions for the presentation of the paper. This work was supported in part by the Natural Science Foundation of China (grants 10773024, 10833002, 10821302, and 10825314), the National Basic Research Program of China (973 Program 2009CB824800), and the CAS/SAFEA International Partnership Program for Creative Research Teams.

REFERENCES

- Abramowicz, M.A. et al. 1995, *ApJ*, 438, L37
 Balbus S.A., & Hawley, J.F. 1998, *Rev. Mod. Phys.*, 70, 1
 Beer, M. E. & Podsiadlowski, P. 2002, *MNRAS*, 331, 351
 Blandford, R. D. & Payne, D. G. 1982, *MNRAS*, 199, 883
 Blandford, R. D. & Znajek, R. L., 1977, *MNRAS*, 179, 433
 Brocksopp, C., et al. 2005, *MNRAS*, 356, 125
 Caballero-Garcia, M. D., et al. 2007, *ApJ*, 669, 534
 Cadolle Bel, M., et al. 2004, *A&A*, 426, 659
 Cadolle Bel, M., et al. 2007, *ApJ*, 659, 549
 Chaty, S., Bessolaz, N. 2006, *A&A*, 455, 639
 Chaty, S. et al. 2003, *MNRAS*, 343, 169
 Corbel, S., Nowak, M. A., Fender, R. P., Tzioumis, A. K., & Markoff, S. 2003, *A&A*, 400, 1007
 Cui, W. et al. 1999, *ApJ*, 512, L43
 Done, C., Gierliński M., & Kubota, A. 2007, *A&ARv*, 15, 1D
 Done, C., & Kubota, A. 2006, *MNRAS*, 371, 1216
 Durant, M., et al. 2008, *ApJ*, 682, L45
 Esin, A. A., McClintock, J. E., & Narayan, R. 1997, *ApJ*, 489, 865
 Esin, A. A., et al. 2001, *ApJ*, 555, 483
 Falcke, H., Kording, E., & Markoff, S. 2004, *A&A*, 414, 895
 Fender, R. 2006, in *Compact Stellar X-Ray Sources*, ed. W.H.G.Lewin & M. van der Klis (Cambridge:Cambridge Univ. Press), 381
 Fender R. P., & Belloni T. M., 2004, *ARA&A*, 42, 317
 Fender R. P., Belloni T. M., & Gallo E., 2004, *MNRAS*, 355, 1105
 Fender, R. P., Gallo, E. & Russell, D. 2010, *MNRAS*, in press (arXiv:1003.5516)
 Frontera F., et al., 2001, *ApJ*, 561, 1006
 Galeev A. A., Rosner R., & Vaiana G. S., 1979, *ApJ*, 229, 318
 Gallo, E., Fender, R. P., & Pooley, G. G. 2003, *MNRAS*, 344, 60
 Giannios, D., & Spruit, H. C. 2004, *A&A*, 427, 251
 Gierlinski, M., Done, C. & Page, K. 2008, *MNRAS*, 388, 753
 Greene, J., Bailyn, C. D., & Orosz, J. A. 2001, *ApJ*, 554, 1290
 Gültekin, K., Cackett, E. M., Miller, J. M., Di Matteo, T., Markoff, S., & Richstone, D. O. 2009, *ApJ*, 706, 404
 Haardt F., & Maraschi L., 1993, *ApJ*, 413, 507
 Hawley, J. F., & Krolik, J. H. 2001, *ApJ*, 548, 348
 Hiemstra, B., Soleri, P., Méndez, M., Belloni, T., Mostafa, R., & Wijnands, R. 2009, *MNRAS*, 394, 2080
 Hirose, S., Krolik, J. H., & Stone, J.M. 2006, *ApJ*, 640, 901
 Hjellming R. M., & Rupen M. P., 1995, *Nature*, 375, 464
 Ho, L. 2002, in *ASP Conf. Ser. 258, Unification of Active Galactic Nuclei*, ed. R. Maiolino, A. Marconi, & N. Nagar (San Francisco, CA: ASP), 165
 Ichimaru S., 1977, *ApJ*, 214, 840
 Igumenshchev I. V., & Abramowicz M. A., 1999, *MNRAS*, 303, 309
 Joinet, A., Kalemci, E., & Senziani, F. 2008, *ApJ*, 679, 655
 Kanbach, G. et al. 2001, *Nature*, 414, 180
 Kubota, A., & Done, C. 2004, *MNRAS*, 353, 980
 Liang, E.P.T. & Price, R.H. 1977, *ApJ*, 218, 247
 Liu, B. F., Yuan, W., Meyer, F., Meyer-Hofmeister, E., & Xie, G. Z. 1999, *ApJ*, 527, L17
 Liu, B.F. et al. 2007, *ApJ*, 671, 695
 Maccarone, T.J. 2005, *MNRAS*, 360, L68
 Maitra, D., Markoff, S., Brocksopp, C., Noble, M., Nowak, M., & Wilms, J. 2009, *MNRAS*, 398, 1638
 Malzac, J., Belmont, R., & Fabian, A.C. 2009, *MNRAS*, 400, 1512
 Malzac, J., Merloni, A., & Fabian, A. C. 2004, *MNRAS*, 351, 253
 Manmoto, T. & Kato, S. 2000, *ApJ*, 538, 295
 Markoff, S., Falcke, H., & Fender, R. 2001, *A&A*, 372, L25
 Markoff, S., Nowak, M.A., & Wilms, J. 2005, *ApJ*, 635, 1203
 McClintock, J. E., & Remillard, R. A. 2006, in *Compact Stellar X-Ray Sources*, ed. W. H. G. Lewin & M. van der Klis, (Cambridge: Cambridge Univ. Press), 157
 Merloni, A., Heinz, S., & di Matteo, T. 2003, *MNRAS*, 345, 1057
 Migliari, S., et al. 2007, *ApJ*, 670, 610
 Miller, J. M., Homan, J., & Miniutti, G. 2006, *ApJ*, 652, L113
 Narayan, R., & McClintock, J.E. 2008, *New Astron. Rev.*, 51, 733
 Narayan, R., & Yi, I. 1994, *ApJ*, 428, L13
 Narayan, R., & Yi, I. 1995, *ApJ*, 452, 710
 Orosz, J. A.; Bailyn, C. D. 1997, *ApJ*, 477, 876
 Ramadevi, M. C., & Seetha, S. 2007, *MNRAS*, 378, 182
 Rees M. J., Phinney E. S., Begelman M. C., & Blandford R. D., 1982, *Nature*, 295, 17
 Rezzolla, L., Yoshida, S'i., Maccarone, T. J., & Zanotti, O. 2003, *MNRAS*, 344, L37
 Różańska, A. & Czerny, B. 2000, *A&A*, 360, 1170
 Shaposhnikov, N., et al. 2007, *ApJ*, 655, 434
 Sharma, P., Quataert, E., Hammett, G. W., & Stone, J. M. 2007, *ApJ*, 667, 714
 Stone J. M., Pringle J. E., & Begelman M. C., 1999, *MNRAS*, 310, 1002
 Stone J. M., & Pringle J. E., 2001, *MNRAS*, 322, 461
 Taam, R. et al. 2008, *ApJ*, 688, 527
 Tchekhovskoy, A., Narayan, R., & McKinney, J.C. 2010, *ApJ*, 711, 50
 Wu, Q. W., Yuan, F., & Cao, X. W. 2007, *ApJ*, 669, 96
 Xie, F.G., Niedzwiecki, A., Zdziarski, A.A., & Yuan, F. 2010, *MNRAS*, 403, 170
 Xue, Y. Q., & Cui, W. 2007, *A&A*, 466, 1053
 Yuan, F. 2003, *ApJ*, 594, L99
 Yuan, F. 2007, in *ASP Conf. Ser. 373, The Central Engine of Active Galactic Nuclei*, ed. L. C. Ho & J.-M. Wang, (San Francisco, CA: ASP), 95
 Yuan, F. & Bu, D. 2010, arXiv:2010.3571
 Yuan, F., & Cui, W. 2005, *ApJ*, 629, 408
 Yuan, F., Cui, W., & Narayan, R. 2005, *ApJ*, 620, 905 (YCN05)
 Yuan, F., Lin, J., Wu, K., & Ho, L.C. 2009a, *MNRAS*, 395, 2183
 Yuan, F. & Narayan, R. 2004, *ApJ*, 612, 724
 Yuan, F., Quataert, E., & Narayan, R. 2003, *ApJ*, 598, 301
 Yuan, F., Xie, F.G., & Ostriker, J.P. 2009b, *ApJ*, 691, 98
 Yuan, F., Yu, Z.L., & Ho, L.C. 2009c, *ApJ*, 703, 1034
 Yuan, F., Zdziarski, A. A., Xue, Y. Q., & Wu, X. B. 2007, *ApJ*, 659, 541
 Zdziarski, A.A. & Gierlinski 2004, *Prog. Theor. Phys. Suppl.*, 155, 99
 Zdziarski A. A., Lubinski P., Gilfanov M., & Revnivtsev M., 2003, *MNRAS*, 342, 355
 Zhang, G. B., Qu, J. L., Zhang, S., Zhang, C. M., Zhang, F., Chen, W., Song, L. M., & Yang, S. P. 2007, *ApJ*, 659, 1511